Fracture Toughness of Carbon Foam

S. CHOI AND B. V. SANKAR*
Department of Mechanical & Aerospace Engineering
University of Florida
Gainesville, FL 32611, USA

(Received February 11, 2003)

ABSTRACT: Mode I fracture toughness of open cell carbon foam was measured using single edge notched four-point bend specimens. A micromechanical model was developed assuming a rectangular prism as the unit-cell. A small region surrounding the crack tip was modeled using finite elements. Displacement boundary conditions were applied to the boundary of the region based on linear elastic fracture mechanics for orthotropic materials. From the finite element results the Mode I stress intensity factor that will cause failure of a crack tip element was determined and it was taken as the predicted fracture toughness of the foam. A simpler model in which the foam consisted of struts of square cross section was also considered. The micromechanical simulations were used to study the variation of fracture toughness as a function of solidity of the foam. The good agreement between the finite element and experimental results for fracture toughness indicates that micromechanics can be an effective tool to study crack propagation in cellular solids.

KEY WORDS: carbon foam, cellular solids, finite element method, fracture toughness, micromechanics, orthotropic material.

INTRODUCTION

CELLULAR MATERIALS ARE made up of a net work of beam/plate like structures leaving an open space or cell in between. An excellent treatise on the structure and properties of cellular solids has been presented by Gibson and Ashby [1]. Foams are a class of cellular solids and have been found to be ideal core materials for sandwich construction. Most of the foams currently used are derived from polymeric materials. However there has been a growing interest in metal foams and carbon foams. Carbon foam has great potential in aerospace application because of their thermal resistance, low density, impact damage tolerance, and cost effectiveness. Some of the applications of carbon foam are in heat exchangers and thermal protection systems. While analytical methods for determining the thermal and mechanical properties of cellular materials such as carbon foam are well documented, research on fracture behavior of various foams is still at infancy. Gibson and

*Author to whom correspondence should be addressed. E-mail: sankar@ufl.edu

0021-9983/03/23 2101–16 $10.00/0 DOI: 10.1177/002199803036264

Ashby [1] have presented approximate formulas for Mode I fracture toughness of cellular solids in terms of their relative density and tensile strength. These are limited to cracks parallel to the principal material direction. Also, fracture behavior under mixed mode has not been studied. Choi and Sankar [2] have developed finite element based micromechanics methods as well as analytical methods for predicting Mode I, Mode II, and mixed mode fracture toughness of cellular solids. They also studied cracks inclined at an angle to the principal material direction. In the present study, the Mode I fracture toughness of carbon foam was measured experimentally using single edge notched bend specimens. In addition to the experimental approach, a finite element based micromechanics has been developed to predict the fracture toughness. The agreement between the test results and numerical results are good, indicating micromechanics can be a powerful tool in predicting the fracture behavior of foams and other cellular solids.

From the SEM image of a low-density carbon foam shown in Figure 1, one can note that the cells are irregularly sized and spaced. The cell size is measured to be in the range of 1–2 mm. Some of the mechanical properties of this particular carbon foam as reported by Touchstone Research Laboratory, Inc. [2], manufacturers of the foam, are shown in Table 1. The solidity (relative density) is determined by dividing, ρ^*, density of the foam, by ρ_s, the density of solid carbon that makes the cell walls. The densities of various forms of carbon are given in Table 2. The solidity of the carbon foam used in the present study was

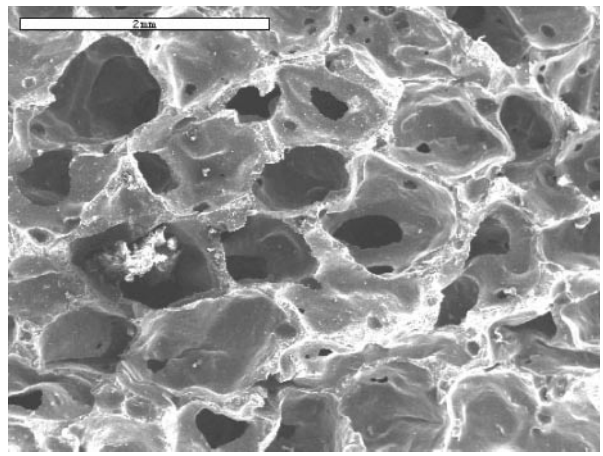

Figure 1. *SEM image of low-density carbon foam.*

Table 1. Mechanical properties of carbon foam.

Elastic modulus (***E****)	123.79 MPa
Tensile strength (σ_u^*)	3.5805 MPa
Density (ρ^*)	295.3 kg/m^3

Table 2. Densities of various forms of carbon.

Diamond (C wt.%100)	3510 kg/m^3
Graphite carbon fiber (C wt.%100)	2250 kg/m^3
Zoltec Pane 30 MF carbon fiber (C wt.% 99.5)	1750 kg/m^3

based on the value of solid density $\rho_s = 2250\,\text{kg/m}^3$, and the solidity is determined as 0.1312.

FRACTURE TESTS

There are several methods available for measuring the fracture toughness of cellular materials. Compact tension test (CT), Single edge notched bend test (SENB), and Double edge notched tension test (DENT) performed by Fowlkes [6] are some of the tests that are suitable for foam materials. In the present study, we chose the single edge notched four-point bend specimens for measuring the fracture toughness of carbon foams. It was thought that the four-point bending test would yield more accurate and repeatable results as the crack is in a region under constant bending moment and that has no transverse shear force. Hence small offset of the loading point with respect to the crack location will not significantly affect the results.

The specimen dimensions are depicted in Figure 2. The height of the specimen was about 50 mm and the crack length was about 25 mm. Individual specimen dimensions are given in Table 3. A notch was cut using a diamond saw, and then a razor blade was used to sharpen the crack tip. The crack length was the distance of the crack tip from the bottom surface of the beam. The tests were conducted under displacement control in a material testing machine at the rate of 0.5 mm/min (Figure 3). Load–deflection diagrams are given in Figure 4. It may be noted from the curves that the crack propagated instantaneously and the specimens failed in a brittle manner. The fracture loads for various specimens are

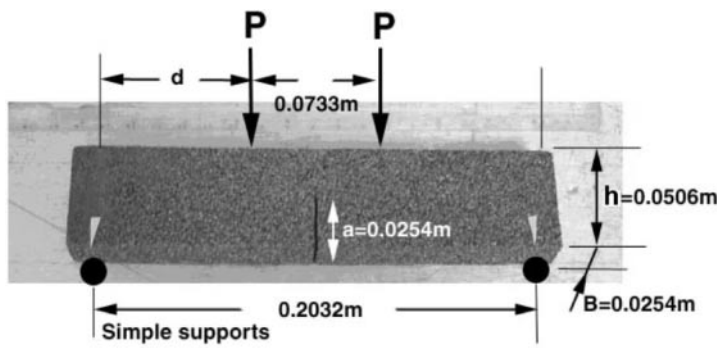

Figure 2. *SENB specimen geometry.*

Table 3. Dimensions and experimental results for fracture toughness for various specimens.

Specimen	Span *L* (m)	Height *h* (m)	Width *B* (m)	Crack Length *a* (m)	Density (kg/m^3)	Fracture Load (N)	K_{IC} (MPa m$^{1/2}$)
IF06	0.2284	0.0512	0.0255	0.0264	284	100.9	0.1315
IF07	0.2291	0.0500	0.0255	0.0252	301	112.0	0.1458
IF09	0.2290	0.0507	0.0255	0.0259	292	92.54	0.1201
IF10	0.2290	0.0506	0.0256	0.0261	297	105.8	0.1372
3 Pt. bending	0.2282	0.0504	0.0255	0.0250	302	63.29	0.1173

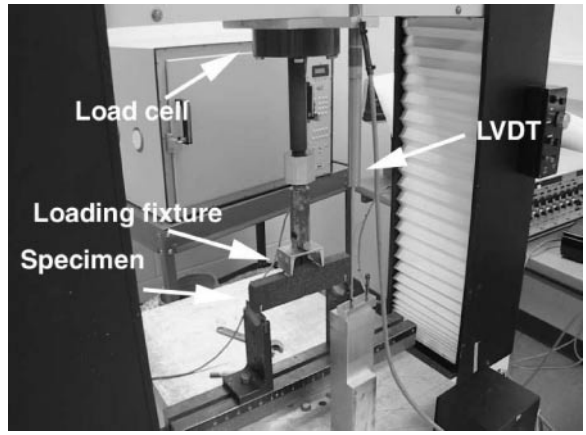

Figure 3. *Four-point bending test setup on a material testing machine.*

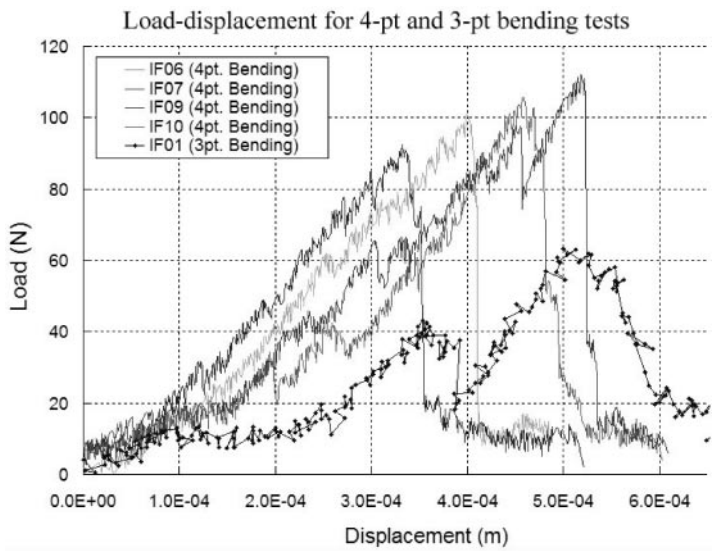

Figure 4. *Load–displacement curves of four-point bending tests on carbon foam.*

listed in Table 3. The Mode I fracture toughness was calculated from the load at failure using the following formula [3]:

$$K_I = \sigma_\infty \sqrt{\pi a}\left(1.12 - 1.39\frac{a}{w} + 7.3\frac{a^2}{w^2} - 13\frac{a^3}{w^3} + 14\frac{a^4}{w^4}\right) \tag{1}$$

where the maximum bending stress σ_∞ in the uncracked beam is determined from the bending moment at the center of the beam using the simple beam theory formula as

$$\sigma_\infty = \frac{6M}{Bw^2} \tag{2}$$

In Equation (2), M is the constant bending moment in the central region, h is the height of the specimen and B is the width. The bending moment M is given by $M = Pd/2$, where d is the distance between one of the top loading points and the corresponding bottom support as shown in Figure 2. The results for fracture toughness are listed in Table 3. For the carbon foam samples tested, the average Mode I fracture toughness is found to be $0.1337\,\text{MPa}\,\text{m}^{1/2}$ with a standard deviation of $0.011\,\text{MPa}\,\text{m}^{1/2}$ (about 8%).

FINITE ELEMENT SIMULATIONS

Unit-cell Model and Solid Properties

The first step in simulating the crack propagation in carbon foam is to idealize the microstructure of the foam. The unit-cell is assumed as a perfect cube of side c in Figure 5. The foam model is created by placing a spherical void (bubble) at the center of the cube. By varying the radius of the bubble R, foams of various solidities can be modeled. A relation between the solidity and the R/c ratio is derived as follows (see Appendix A):

$$\frac{\rho^*}{\rho_s} = \frac{4+\pi}{4} + \frac{8}{3}\pi\left(\frac{R}{a}\right)^3 - 3\pi\left(\frac{R}{a}\right)^2$$

The average dimension of the unit-cell was obtained from the SEM images of the cross section of carbon foam. Then, the radius of the spherical void can be determined from the solidity of the foam. The Pro/Engineering®, modeling application, was used to model the unit-cell and calculate the solid volume. In the present study, the unit-cell dimension c is taken as 1.8 mm and the solidity as 0.1312. The Young's modulus and tensile strength of the solid carbon are required in the simulation of fracture. An ideal method of determining the in situ properties of solid carbon is to use advanced experimental techniques such as nano indentation. However, in the current study these properties are inverse-calculated from the overall mechanical properties of the carbon foam measured experimentally. The procedure for determining the Young's modulus and tensile strength of the solid carbon is as follows.

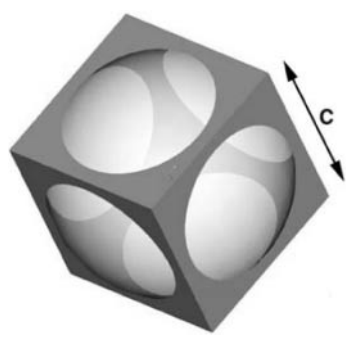

Figure 5. *Unit-cell of solid model.*

The strength of the solid carbon in the foam can be easily estimated from the tensile strength of the carbon foam, which is measured experimentally. The relation between the foam tensile strength and the solid carbon strength is given by

$$\sigma_{\text{us}} = \sigma_u^* \frac{c^2}{A_{\min}} \tag{3}$$

where c is the unit-cell dimension and $A_{\min}$ is the minimum cross sectional area of the struts in the carbon foam normal to the principal material axis. It should be noted that the tensile strength of the foam is for a direction parallel to one of the principal material axes. The area $A_{\min}$ was obtained from the modeling software and it was equal to $= 7.146 \times 10^{-8}\,\text{mm}^2$. Substituting the dimensions of the unit-cell and the measured carbon foam tensile strength ($\sigma_u^* = 3.58$ MPa), the strength of solid carbon was estimated as 162 MPa.

The Young's modulus E_{s} of solid carbon was estimated by a trial and error method. An initial value for E_{s} is assumed and the elastic constants of the carbon foam are determined by using the micromechanical methods developed by Sankar et al. [6]. Then the value of E_{s} can be scaled to match the micromechanical results for E^* to the experimentally measured E^*. The unit-cell was modeled using 4-noded tetrahedral solid elements. Due to symmetry only a portion of the unit-cell was modeled and periodic boundary conditions were imposed such that only one of the macrostrains is nonzero [6]. We assume a value for E_{s} and ν_{s}, and the forces required to deform the unit cell are calculated from the nodal reactions. From the forces the macrostresses can be computed. For example, the macro stress σ_x^* and σ_y^* can be derived as

$$\sigma_x^* = \frac{\sum F_x}{c^2}, \qquad \sigma_y^* = \frac{\sum F_y}{c^2} \tag{4}$$

where ΣF_x represents the sum of all nodal forces on a face normal to the x-axis and ΣF_y is the sum of all the nodal forces F_y on the face normal to the y-axis.

The carbon foam is assumed as an orthotropic material and the macrostresses and strains are substituted in the constitutive relation to obtain the compliance coefficients S_{ij}. From the S matrix the elastic constants can be estimated using the following relations:

$$\begin{Bmatrix} \varepsilon_x^* \\ \varepsilon_y^* \\ \varepsilon_z^* \end{Bmatrix} = \begin{Bmatrix} S_{11} & S_{12} & S_{12} \\ S_{12} & S_{11} & S_{12} \\ S_{12} & S_{12} & S_{11} \end{Bmatrix} \begin{Bmatrix} \sigma_x^* \\ \sigma_y^* \\ \sigma_z^* \end{Bmatrix} \quad \begin{Bmatrix} \frac{1}{E_x} & -\frac{\nu_{yx}}{E_y} & -\frac{\nu_{zx}}{E_z} \\ -\frac{\nu_{xy}}{E_x} & \frac{1}{E_y} & -\frac{\nu_{zy}}{E_z} \\ -\frac{\nu_{xz}}{E_x} & \frac{\nu_{yz}}{E_y} & \frac{1}{E_z} \end{Bmatrix} = \begin{bmatrix} S_{11} & S_{12} & S_{12} \\ S_{12} & S_{11} & S_{12} \\ S_{12} & S_{12} & S_{11} \end{bmatrix} \tag{5}$$

The FE model contained approximately 100,000 solid tetrahedral elements. A displacement $u_y = 1$ was applied to the top surface of a unit-cell (Figure 6). The contour plot of maximum principal stresses is shown in Figure 6.

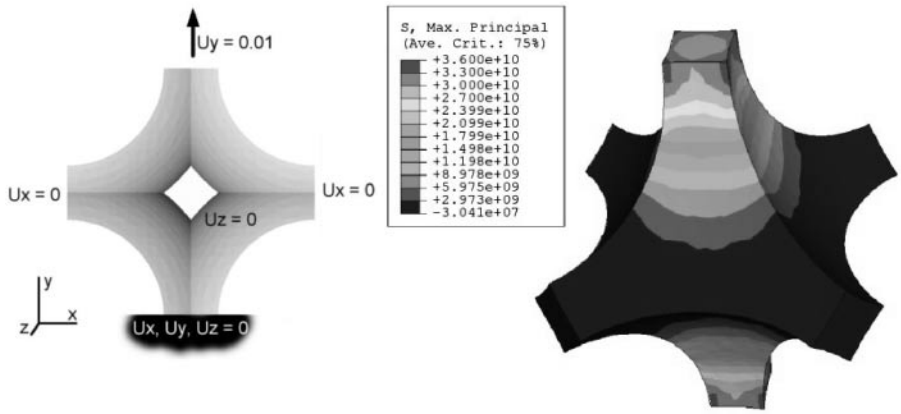

Figure 6. *Boundary conditions on the unit-cell surfaces and maximum principal stress distribution when the unit-cell is stretched in the y-direction.*

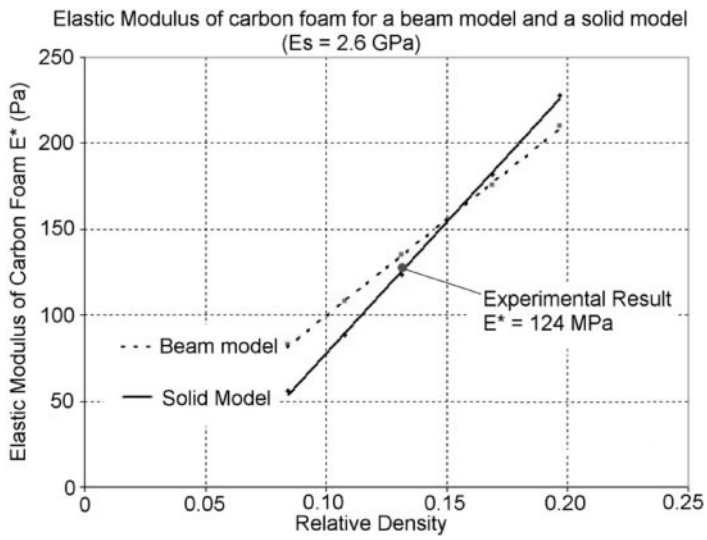

Figure 7. *Elastic modulus E^* as a function of relative density (solidity) for $E_s = 2.6$ GPa. Results from solid model and beam model are presented.*

For the sake of simplicity no attempt was made to estimate the Poisson's ratio ν_s using the micromechanical method and it was assumed to be equal to 0.17 based on a previous study [2]. Based on the foam properties given in Table 1 and the unit-cell size c of 1.8 mm, the Young's modulus of solid carbon E_s was estimated to be 2.6 GPa. Using this value for E_s the Young's modulus of carbon foams for various solidity values was calculated using the FE model and they are referred to as "solid model" in Figure 7. Another simpler model called "beam model" was also developed as described in the next section. The shear modulus in the principal material coordinates was also calculated using the micromechanics analysis developed by Sankar and Marrey [6]. The variation of shear modulus as a function of solidity is shown in Figure 8.

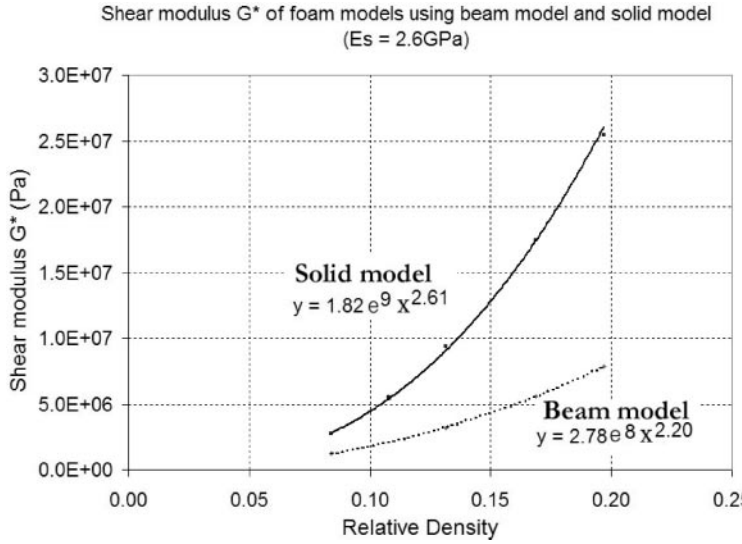

Figure 8. *Shear modulus G^* as a function of relative density (solidity) for $E_s = 2.6$ GPa. Results from solid model and beam model are presented.*

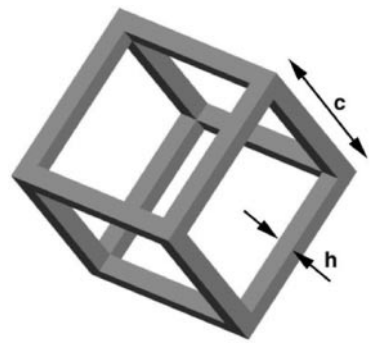

Figure 9. *Unit-cell of beam model.*

Beam Model

In addition to the solid model described in the preceding section, a simple lattice model was also attempted. In this model the foam is assumed to be made up of struts arranged in a cubic lattice pattern. The length of the strut was equal to the unit-cell dimension c (see Figure 9). The struts were assumed to be beams of uniform square cross section, and their dimensions were determined from the solidity of the foam. The wall thickness h of carbon foam is determined by using the equation for relative density as follows [2]:

$$\frac{\rho^*}{\rho_s} = 3\left(\frac{h}{c}\right)^2 - 2\frac{h^3}{c^3} \tag{6}$$

From Equation (6) above, the wall thickness h is determined to be 0.4086 mm for a solidity of 0.1312 and $c = 1.8$ mm. Since the beam model is composed of uniform beam elements, finite element methods are not necessary to determine the relation between the solid properties and foam properties. Analytical expressions for various elastic properties have been derived earlier [2], and the results are as follows:

$$E_s = \left(\frac{c}{h}\right)^2 E^* \tag{7}$$

$$G^* = \frac{1}{2} E_s \left(\frac{h}{c}\right)^4 \tag{8}$$

The relation between the strength of the foam (σ_u^*) and the solid strut strength (σ_{us}) is given by

$$\sigma_{us} = \left(\frac{c}{h}\right)^2 \sigma_u^* \tag{9}$$

Based on the Equations (7) and (9), the Young's modulus E_s and the strength σ_{us} are found to be 2.4 and 69.5 MPa, respectively. The variation of E^* and G^* with the solidity for the beam model are shown in Figures 7 and 8, respectively.

Fracture Toughness Estimation using the Solid Model

In this section, we describe a finite element based-micromechanics model to estimate the fracture toughness of the cellular solid. The crack is assumed to be parallel to one of the principal material axes. The crack is created by breaking the ligaments of the unit-cell (Figure 10). To determine the fracture toughness, a small region of the foam around the crack tip is modeled using finite elements. Only Mode I fracture is

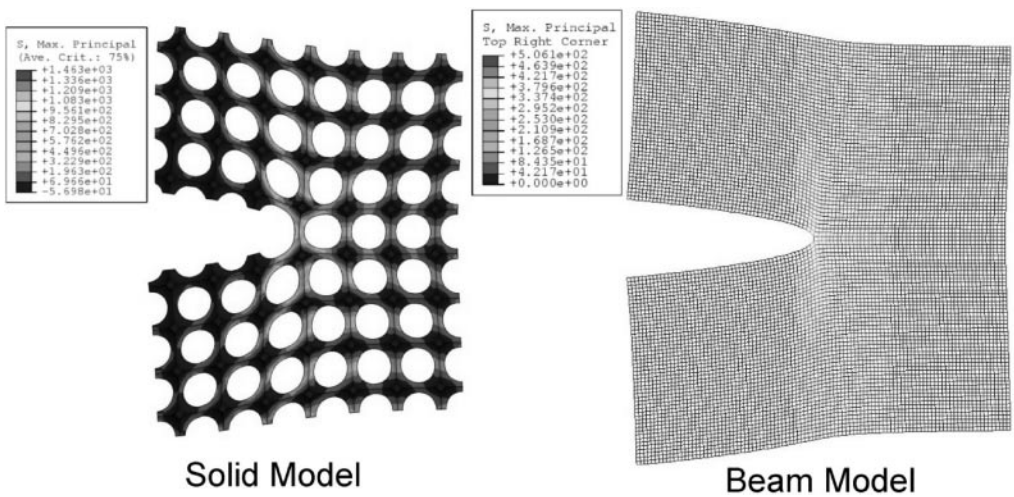

Figure 10. *Maximum principal stress distribution of solid and beam models for a unit K_I at the crack tip.*

considered in the present study. The boundary of the cellular solid is subjected to displacement boundary conditions (u_x and u_y) corresponding to a unit K_I, i.e., $K_I = 1$. The displacement components in the vicinity of a crack tip in an orthotropic solid can be found in [4] and they are as follows:

$$u_x = K_I\sqrt{\frac{2r}{\pi}}\mathrm{Re}\left\{\frac{1}{s_1 - s_2}\left[s_1 p_2(\cos\theta + s_2\sin\theta)^{1/2} - s_2 p_1(\cos\theta + s_1\sin\theta)^{1/2}\right]\right\}$$
$$u_y = K_I\sqrt{\frac{2r}{\pi}}\mathrm{Re}\left\{\frac{1}{s_1 - s_2}\left[s_1 q_2(\cos\theta + s_2\sin\theta)^{1/2} - s_2 q_1(\cos\theta + s_1\sin\theta)^{1/2}\right]\right\} \quad (10)$$

The parameters s_1, s_2, p_1, p_2, q_1, and q_2 depend on the orthotropic material constants, and they are described in Appendix B. The maximum tensile stress in the unit-cells corresponding to unit stress intensity factor is calculated from the FE model. In the case of solid model the maximum stress is obtained as an output of the FE program. From the result the value of K_I that will cause rupture of the strut is estimated, which is then taken as the fracture toughness of the cellular solid.

The solid model used 42 cells with 135,000 solid tetrahedral elements as shown in Figure 10. A contour plot of maximum principal stress is shown in Figure 10. When unit K_I was applied to the crack tip, maximum principal stress σ_{max} was found equal to 1463 Pa. Then the fracture toughness is obtained from the strength of the solid carbon ($\sigma_{us} = 162$ MPa) as

$$K_{IC} = \frac{\sigma_{us}}{\sigma_{max}} = 0.11\ \mathrm{MPa\,m^{1/2}} \quad (11)$$

Comparing the result for fracture toughness given in Equation (11) with the experimental results (Table 3), one can note that the difference is about 16%. Considering the idealizations made in the model and variations in the unit-cell shape and dimensions and in situ properties of the carbon cell walls, the finite element results seem to be reasonable.

The FE model was used to study the variation of fracture toughness with relative density and the resulting relationship is shown in Figure 11. Gibson and Ashby [1] provide an analytical formula for fracture toughness of open-cell foam as given below:

$$\frac{K^*_{IC}}{\sigma_{us}\sqrt{\pi c}} = 0.65\left(\frac{\rho^*}{\rho_s}\right)^{3/2} \quad (12)$$

using the above formula the fracture toughness for the carbon foam considered in this study can be obtained as $0.162\ \mathrm{MPa\,m^{1/2}}$. The variation of K_{IC} according to (12) is presented in Figure 11.

Fracture Toughness using the Beam Model

The procedure for simulating fracture using the beam model is the same as that for the FE solid model. The beam model of carbon foam (Figure 10) consisted of 10,000 cells

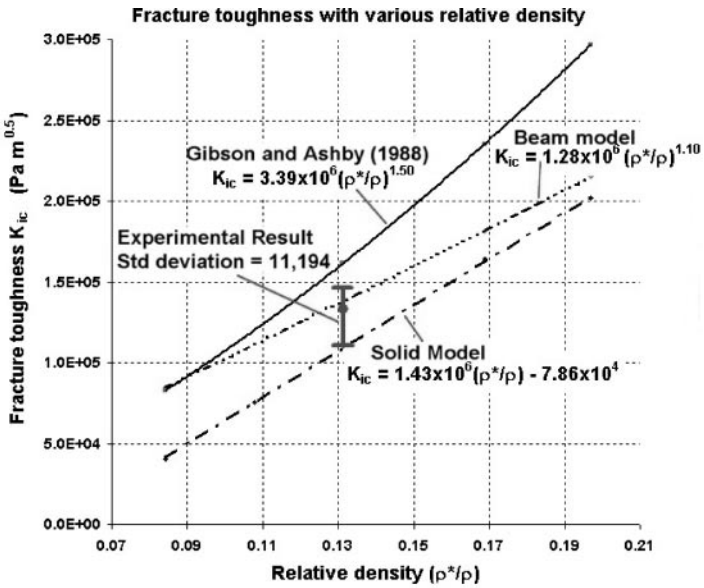

Figure 11. *Variation of fracture toughness of carbon foam with relative density.*

using approximately 20,000 beam elements. When using the beam model, the rotational degree of freedom at each node of the beam element on the boundary of the solid is left as unknown and no couples are applied at these nodes. The maximum principal stress distribution in the beam model for $K_I = 1$ is shown in Figure 10. The maximum principal stress σ_{max} for a unit K_I was found to be equal to 506 Pa. Therefore, the fracture toughness can be estimated as

$$K_{IC} = \frac{\sigma_{us}}{\sigma_{max}} = 0.137\,\text{MPa}\,\text{m}^{1/2} \tag{13}$$

The difference between the experimental result and that from the beam model is only 3%. The beam model was also used to study the variation of fracture toughness with the solidity and it is presented in Figure 11.

CONCLUSIONS

Four-point bend tests were performed on SENB specimens made of carbon foam, and their Mode I fracture toughness was measured. Two micromechanical models were developed to simulate Mode I fracture. Both models assumed a cube as the unit-cell of the foam. In the first model solid finite elements were used to model the foam. The measured density of the carbon foam was used in determining the void size in the micromechanical model. Young's modulus and tensile strength of the solid carbon were also determined from the corresponding values of the carbon foam measured experimentally. A small region surrounding the crack tip was modeled using finite elements. The crack was assumed parallel to one of the principal material directions. Boundary displacements were calculated using linear elastic fracture mechanics for orthotropic materials. From the FE

simulation the stress intensity factor K_I that will cause the failure of the crack-tip elements was determined, and this was taken as the fracture toughness of the cellular material. Good agreement between FE and experimental results indicates that micromechanics simulations can be successfully used to study crack propagation in cellular solids. Future work will focus on mixed mode fracture and crack propagation at an angle to the principal material direction.

APPENDIX A

Analytical Method to Estimate the Solidity of the Foam

We assume that the unit-cell of the cellular material is a cube and the voids are created by placing a spherical bubble at the center of the cube. To estimate the solidity of the foam, the volume of the portion of the sphere contained inside the cube needs to be determined. This can be obtained by subtracting the volume of the sphere outside the unit cell from the total volume of the sphere. The sphere outside the unit cell consists of six domes one on each face of the cube. The volume V_A (see Figure A1) is obtained as

$$V_A = \frac{\psi}{3} R^3 \tag{A1}$$

where ψ is solid angle, which is determined as described below.

From the definition of solid angle we obtain the following relations (see Figure A2):

$$d\psi = \frac{dA}{R^2}$$

$$dA = 2\pi r dr \cos\theta$$

$$\cos\theta = \frac{h}{(h^2 + r^2)^{3/2}}$$

Using the above relations we obtain

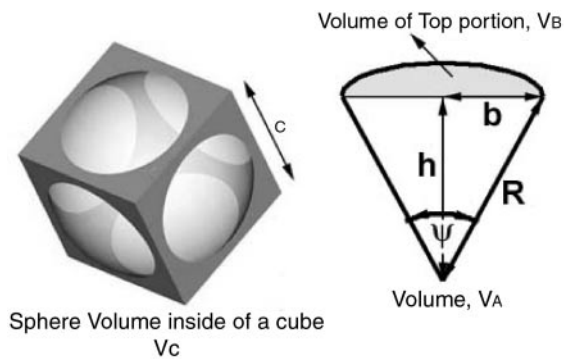

Figure A1. *Unit-cell of solid model.*

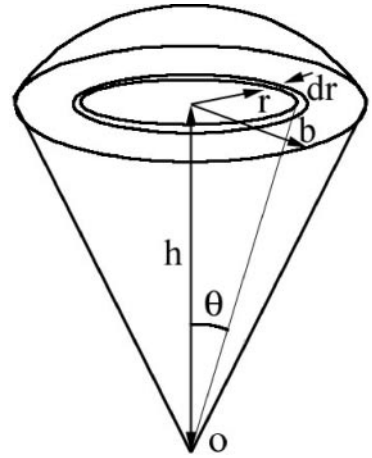

Figure A2. *Definition of solid angle* ψ.

$$d\psi = \frac{2\pi r h dr}{(h^2 + r^2)^{3/2}}$$

Integrating both sides we obtain,

$$\psi = \int_0^b \frac{2\pi\, r\, h\, dr}{(h^2 + r^2)^{3/2}} = 2\pi h\left[\frac{1}{h} - \frac{1}{R}\right] \tag{A2}$$

In deriving (A2) we have used the relation $b^2 = \left(R^2 - h^2\right)$. By substituting Equation (A1) into Equation (A2), V_A is obtained as follows:

$$V_A = \frac{2\pi\, R^2}{3}[R - h] \tag{A3}$$

The volume of the top portion V_B can be obtained by subtracting the volume of the cone from V_A

$$\begin{aligned} V_B &= \frac{2\pi\, R^2}{3}[R - h] - \frac{1}{3}\pi b^2 h \\ &= \frac{2\pi R^3}{3} - \pi R^2 h + \frac{1}{3}\pi h^3 \end{aligned} \tag{A4}$$

The volume V_C of portion the sphere inside the unit-cell is given by

$$\begin{aligned} V_C &= \frac{4\pi R^3}{3} - 6V_B \\ &= -\frac{8\pi R^3}{3} + 3\pi R^2 c - \frac{\pi c^3}{4} \end{aligned} \tag{A5}$$

In Equation (A5) we have used the fact $c = 2h$.

The solidity of the foam is defined as the volume fraction of the solid in the unit-cell. It is also the ratio of the foam density and the solid density of the foam material, viz., carbon in the present case.

$$\begin{aligned}\frac{\rho^*}{\rho_s} &= \frac{c^3 - V_c}{c^3} \\ &= 1 - \frac{1}{c^3}\left[-\frac{8\pi R^3}{3} + 3\pi R^2 c - \frac{1}{4}\pi c^3\right]\end{aligned} \tag{A6}$$

For an open cell foam, Equation (A6) is only valid in the range $c/2 \le R \le c/\sqrt{2}$

Equation (A6) can also be written in terms of the aspect ratio R/c as

$$\frac{\rho^*}{\rho_s} = \frac{4+\pi}{4} + \frac{8}{3}\pi\left(\frac{R}{c}\right)^3 - 3\pi\left(\frac{R}{c}\right)^2 \tag{A7}$$

APPENDIX B

Crack Tip Displacement Fields for Orthotropic Materials

The open-cell foam is considered as an orthotropic material. The principal material directions are parallel to the 1 and 2 axes. The stress–strain relations in the 1–2 plane for the case of plane strain can be expressed as

$$\begin{Bmatrix} \varepsilon_1 \\ \varepsilon_2 \\ \gamma_{12} \end{Bmatrix} = [S]\{\sigma\} = \begin{bmatrix} \frac{1}{E^*} & -\frac{v}{E^*} & 0 \\ -\frac{v}{E^*} & \frac{1}{E^*} & 0 \\ 0 & 0 & \frac{1}{G^*} \end{bmatrix} \begin{Bmatrix} \sigma_1 \\ \sigma_2 \\ \tau_{12} \end{Bmatrix} \tag{B1}$$

When the cellular model is oriented to an angle with the principal material axes, the stress–strain relation can be transformed from the 1–2 plane to the x–y plane by using transformation matrix $[T]$. The angle θ is taken positive when the angle of the 1–2 directions are measured from x–y directions.

$$[T] = \begin{bmatrix} \cos^2\theta & \sin^2\theta & 2\sin\theta\cos\theta \\ \sin^2\theta & \cos^2\theta & -2\sin\theta\cos\theta \\ -\sin\theta\cos\theta & \sin\theta\cos\theta & \cos^2\theta - \sin^2\theta \end{bmatrix} \tag{B2}$$

$$\begin{Bmatrix} \sigma_x \\ \sigma_y \\ \sigma_z \end{Bmatrix} = [T] \begin{Bmatrix} \sigma_1 \\ \sigma_2 \\ \sigma_3 \end{Bmatrix} \tag{B3}$$

By applying the transformation matrix, the compliance matrix in the x–y plane $[\bar{S}]$ is written as

$$\begin{Bmatrix} \varepsilon_x \\ \varepsilon_y \\ \gamma_{sy} \end{Bmatrix} = [T]^T[S][T] \begin{Bmatrix} \sigma_x \\ \sigma_y \\ \tau_{xy} \end{Bmatrix} = \begin{Bmatrix} \overline{S}_{11} & \overline{S}_{12} & \overline{S}_{16} \\ \overline{S}_{12} & \overline{S}_{22} & \overline{S}_{26} \\ \overline{S}_{16} & \overline{S}_{26} & \overline{S}_{66} \end{Bmatrix} \begin{Bmatrix} \sigma_x \\ \sigma_y \\ \tau_{xy} \end{Bmatrix} \tag{B4}$$

The components in the $[\bar{S}]$ matrix can be obtained in terms of material properties in 1–2 plane.

$$\begin{aligned}
\overline{S}_{11} &= S_{11}\cos^4\theta + (2S_{12} + S_{66})\sin^2\theta\cos^2\theta + S_{22}\sin^4\theta \\
\overline{S}_{12} &= S_{12}(\sin^4\theta + \cos^4\theta) + (S_{11} + S_{22} - S_{66})\sin^2\theta\cos^2\theta \\
\overline{S}_{22} &= S_{11}\sin^4\theta + (2S_{12} + S_{66})\sin^2\theta\cos^2\theta + S_{22}\cos^4\theta \\
\overline{S}_{16} &= (2S_{11} - 2S_{12} - S_{66})\sin\theta\cos^3\theta - (2S_{22} - 2S_{12} - S_{66})\sin^3\theta\cos\theta \\
\overline{S}_{16} &= (2S_{11} - 2S_{12} - S_{66})\sin^3\theta\cos\theta - (2S_{22} - 2S_{12} - S_{66})\sin\theta\cos^3\theta \\
\overline{S}_{11} &= 2(2S_{11} + 2S_{22} - 4S_{12} - S_{66})\sin^2\theta\cos^2\theta + S_{66}(\sin^4\theta + \cos^4\theta)
\end{aligned} \tag{B5}$$

The characteristic equation of the orthotropic material is given by [4]

$$\overline{S}_{11}\mu^4 - 2\overline{S}_{16}\mu^3 + \left(2\overline{S}_{12} + \overline{S}_{66}\right)\mu^2 - 2\overline{S}_{26}\mu + \overline{S}_{22} = 0 \tag{B6}$$

where the complex roots of the characteristic equation are given by $\mu_j (j = 1, 2, 3, 4)$.

From the four roots, the two unequal roots with positive conjugate values are denoted by s_1 and s_2:

$$s_1 = \mu_1 = \alpha_1 + i\beta_1 \qquad s_2 = \mu_2 = \alpha_2 + i\beta_2 \tag{B7}$$

The constants p_j and $q_j (j = 1, 2)$ are related to s_1 and s_2 as follows:

$$\begin{aligned}
p_1 &= a_{11}s_1^2 + a_{12} - a_{16}s_1 \qquad & p_2 &= a_{11}s_2^2 + a_{12} - a_{16}s_2 \\
q_1 &= \frac{a_{12}s_1^2 + a_{22} - a_{26}s_1}{s_1} \qquad & q_2 &= \frac{a_{12}s_2^2 + a_{22} - a_{26}s_2}{s_2}
\end{aligned} \tag{B8}$$

The displacement components at points (r, θ) in the vicinity of the crack tip for Mode I can be derived as [4]:

$$\begin{aligned}
u_x &= K_I\sqrt{\frac{2r}{\pi}}\mathrm{Re}\left\{\frac{1}{s_1 - s_2}\left[s_1p_2(\cos\theta + s_2\sin\theta)^{1/2} - s_2p_1(\cos\theta + s_1\sin\theta)^{1/2}\right]\right\} \\
u_y &= K_I\sqrt{\frac{2r}{\pi}}\mathrm{Re}\left\{\frac{1}{s_1 - s_2}\left[s_1q_2(\cos\theta + s_2\sin\theta)^{1/2} - s_2q_1(\cos\theta + s_1\sin\theta)^{1/2}\right]\right\}
\end{aligned} \tag{B9}$$

ACKNOWLEDGMENTS

This research was supported by a grant from Touchstone Research Laboratory, Ltd., Tridelphia, WV, USA. The authors are thankful to Mr. Brian Joseph, COO and Mr. Charlie Rowe, Laboratory Director for their support. Thanks are due to Dr. Ajit Roy of Wright-Patterson Air Force Base for his guidance and technical discussions during the course of this project. Partial support from the NASA URETI Grant NCC3-994 is also acknowledged.

REFERENCES

1. Gibson, L.J. and Ashby, M.F. (1988). *Cellular Solids: Structure and Properties*, **2nd edn**, pp. 219–222, Cambridge University Press, Cambridge, United Kingdom.
2. Choi, S. and Sankar, B.V. (2002). Micromechanical Methods to Predict the Fracture Toughness of Cellular Solids, Technical Report, Department of Mechanical and Aerospace Engineering, University of Florida, PO Box 116250, Gainesville, FL 32611.
3. Hellan, K. (1984). *Introduction to Fracture Mechanics*, p. 244, McGraw-Hill, NY.
4. Sih, G.C. and Liebowitz, H. (1968). Mathematical Theories of Brittle Fracture, In: Liebowitz, H., (ed.), *Fracture – An Advanced Treatise*, Vol. 2, pp. 67–190, Academic Press, New York.
5. W. Charless Fowlkes (1974). Fracture Toughness Tests of a Rigid Polyurethane Foam, *International Journal of Fracture*, **10**(1): 99–108.
6. Marrey, Ramesh V. and Sankar, Bhavani V. (1995). Micromechanical Models for Textile Structural Composites, NASA Contractor Report 198229.